Synthesis of Side-Chain Liquid Crystalline Polyoxetanes Containing 4-(Alkanyloxy)phenyl *trans*-4-Alkylcyclohexanoate Side Groups

Yong-Hong Lu and Chain-Shu Hsu*

Department of Applied Chemistry, National Chiao Tung University, Hsinchu, Taiwan 30050, Republic of China

Received July 5, 1994; Revised Manuscript Received September 21, 1994®

ABSTRACT: The synthesis of side-chain liquid crystalline polyoxetanes containing 4-(alkanyloxy)phenyl *trans*-4-alkylcyclohexanoate side groups is presented. Differential scanning calorimetry, optical polarizing microscopy, and X-ray diffraction measurements reveal polymorphism of mesophases for all obtained polymers. Both spacer length and terminal alkyl length have a profound influence on the nature and thermal stability of the mesophases. Although the polyoxetane backbone is more flexible than the polymethacrylate backbone, side-chain crystallization did not occur for any of the synthesized polymers.

Introduction

Side-chain liquid crystalline polymers (LCPs) are of both theoretical and practical interest because they combine the anisotropic properties of liquid crystals with the polymeric properties and have the potential of being used for some new applications.[1–15] So far, most of the side-chain LCPs have been prepared mainly by radical polymerization of (meth)acrylates and by the hydrosilation of poly(methylhydrosiloxane) backbones with mesogenic olefins. In recent years an increasing amount of research has been directed at synthesizing new well-defined side-chain LCPs by living cationic polymerization,[16] ring-opening polymerization[17–24] and living ring-opening methathesis polymerization.[25–29] Recently, Kawakami et al. reported the first example of side-chain LC polyoxetanes by cationic ring-opening polymerization.[22–24]

In our previous works we reported side-chain LC polysiloxanes containing cyclohexane-based mesogenic side groups which exhibit conformational isomerism.[30,31] These kinds of mesogens can be used to synthesize noncrystallizable side-chain LCPs even when the polymers contain very long spacer units.[32–34] The goal of this paper is to present the synthesis of some new side-chain LC polyoxetanes containing 4-(alkanyloxy)phenyl *trans*-4-alkylcyclohexanoate side groups. The effects of spacer length as well as terminal alkyl length on the properties of mesophases exhibited by the synthesized polymers are discussed.

Experimental Section

Materials. *trans*-4-*n*-Propylcyclohexanoic acid, *trans*-4-*n*-butylcyclohexanoic acid, and *trans*-4-*n*-pentylcyclohexanoic acid were obtained from Tokyo Kaisei Inc. and were used as received. Boron trifluoride ether complex was also purchased from Tokyo Kaisei Inc. and was distilled before use. 3-(Hydroxymethyl)-3-methyloxetane and all other reagents were obtained from Aldrich and were used as received. Dichloromethane used in the ring-opening polymerization was refluxed over calcium hydride and then distilled under nitrogen.

Techniques. ^{1}H NMR spectra (300 MHz) were recorded on a Varian VXR-300 spectrometer. Thermal transitions and thermodynamic parameters were determined by using a Seiko SSC/5200 differential scanning calorimeter equipped with a liquid nitrogen cooling accessory. Heating and cooling rates were 10 °C/min. Thermal transitions reported were collected during the second heating and cooling scans. A Carl–Ziess Axiphot optical polarized microscope equipped with a Mettler FP 82 hot stage and a FP 80 central processor was used to observe the thermal transitions and to analyze the anisotropic textures. Gel permeation chromatography (GPC) was run on an Applied Biosystems 400 LC instrument equipped with a differential refractometer, a UV detector, and a set of PL gel columns of 10^2, 5×10^2, 10^3, and 10^4 Å. The molecular weight calibration curve was obtained by using standard polystyrenes. X-ray diffraction measurements were performed with nickel-filtered Cu Kα radiation with a Rigaku powder diffractometer.

Synthesis of Monomers IM–XIIIM. The synthesis of oxetane monomers IM–XIIIM is outlined in Schemes 1 and 2.

3-[(Tosyloxy)methyl]-3-methyloxetane (1). To the aqueous solution (80 mL of water) of 3-(hydroxymethyl)-3-methyloxetane (9.10 g, 89.2 mmol) and sodium hydroxide (20.0 g, 0.05 mol) was added dropwise the tosyl chloride (23.8 g, 0.125 mol) in tetrahydrofuran (THF, 80 mL), and the mixture reacted overnight at room temperature. After THF was removed under reduced pressure, the product was extracted with diethyl ether three times (150 mL). The crude product was isolated by evaporating the solvent and further purification by recrystallization from *n*-hexane to form white crystals, mp 57.1 °C, yield 88.2%. ^{1}H NMR chemical shifts: δ 1.31 (s, 3H, $-CH_3$), 2.47 (s, 3H, $-Ph-CH_3$), 4.11 and 4.36 (m, 6H, $-CH_2-$OTs and two $-CH_2-$ in the oxetane ring), 7.39 and 7.81 (two d, 4H, aromatic protons).

3-[[(3-Bromopropyl)oxy]methyl]-3-methyloxetane (4), 3-[[(4-Bromobutyl)oxy]methyl]-3-methyloxetane (5), 3-[[(5-Bromopentyl)oxy]methyl]-3-methyloxetane (6), and 3-[[(6-Bromohexyl)oxy]methyl]-3-methyloxetane (7). All four compounds were prepared by the same method. The synthesis of compound **6** is described below.

A two-phase system composed of dibromopentane (70 g, 0.304 mol) in hexane (100 mL) and 3-(hydroxymethyl)-3-methyloxetane (10 g, 0.098 mol), sodium hydroxide (65.0 g, 1.625 mol), and tetrabutylammonium bromide (0.5 g) in water (100 mL) was stirred for 24 h at room temperature and heated to reflux under stirring for 2 h. After the reaction system was cooled to room temperature, water (100 mL) was added, and the

* To whom all correspondence should be addressed.
® Abstract published in *Advance ACS Abstracts,* January 15, 1995.

0024-9297/95/2228-1673$09.00/0

Scheme 1. Synthesis of Monomer IM and Polymer IP

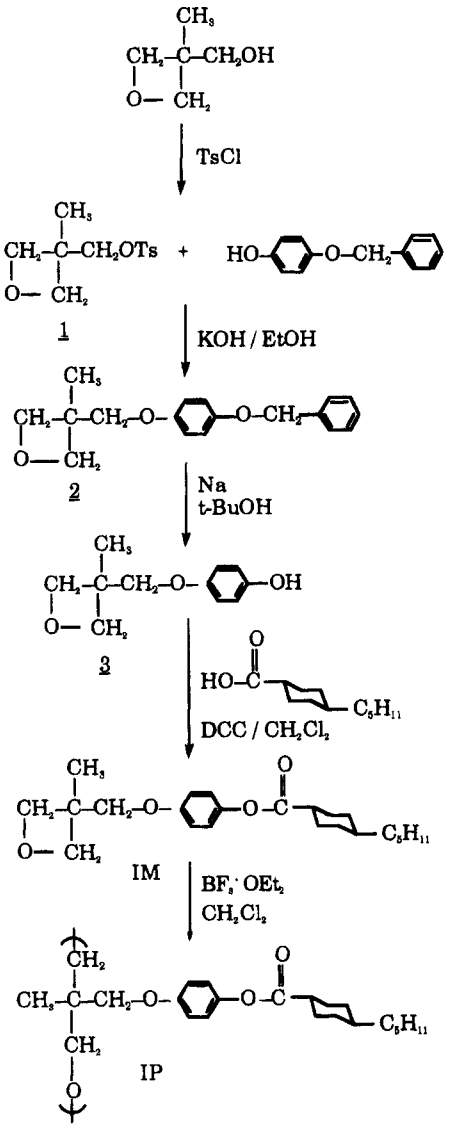

Scheme 2. Synthesis of Monomers IIM–XIIIM and Polymers IIP–XIIIP

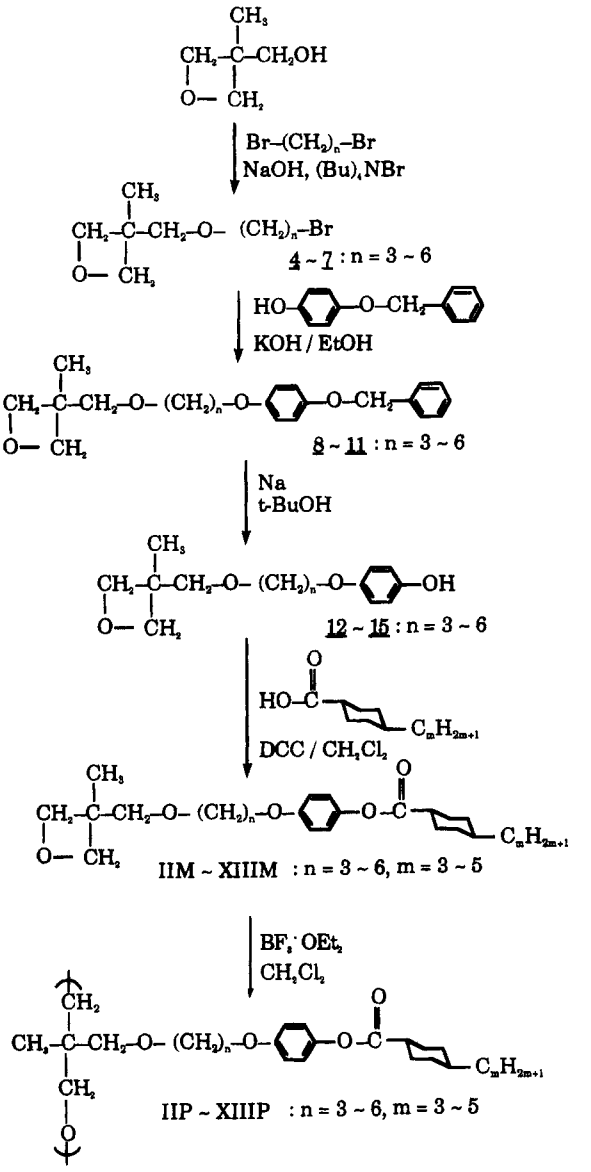

organic layer was extracted three times with hexane. The product was isolated by evaporating the solvent after drying the solution with anhydrous magnesium sulfate. The crude product was purified by distillation, bp 80–85 °C (0.15 mmHg), to yield 18.4 g (75%) of a colorless liquid, bp 80–85 °C (0.15 mmHg). ^{1}H NMR chemical shifts: 1.30 (s, 3H, $-CH_3$), 1.42–1.90 (m, 6H, $-O-CH_2-(CH_2)_3-$), 3.32–3.52 (m, 6H, $-CH_2-O-CH_2-$ and $-CH_2-Br$), 4.33 and 4.50 (two d, 4H, two $-CH_2-$ in the oxetane ring).

3[[[4-(Benzyloxy)phenyl]oxy]methyl]-3-methyloxetane (2), 3-[[[3-[[4-(Benzyloxy)phenyl]oxy]propyl]oxy]methyl]-3-methyloxetane (8), 3-[[[4-[[4-(Benzyloxy)phenyl]oxy]butyl]oxy]methyl]-3-methyloxetane (9), 3-[[[5-[[4-(Benzyloxy)phenyl]oxy]pentyl]oxy]methyl]-3-methyloxetane (10), and 3-[[[6-[[4-(Benzyloxy)phenyl]oxy]hexyl]oxy]methyl]-3-methyloxetane (11). All five compounds were prepared by the same method. The synthesis of compound **10** is described below.

p-(Benzyloxy)phenol (8.55 g, 0.043 mol) was added to a solution of 2.39 g (0.043 mol) of potassium hydroxide in 250 mL (90%) of ethanol. Potassium iodide (0.2 g) was added, and the solution was heated to reflux temperature for 1 h. 3-[[(5-Bromopentyl)oxy]methyl]-3-methyloxetane (**6**) (8.9 g, 0.036 mol) was added slowly, and the solution was heated to reflux temperature and stirred overnight. The solution was cooled, the solid salts were removed by filtration, and ethanol was removed in a rotovap. The remaining solid was extracted with ethyl acetate and washed three times with 10% KOH. The collected ethyl acetate solution was dried over anhydrous magnesium sulfate and evaporated to dryness. The obtained crude product was purified by column chromatography (silica gel, ethyl acetate:*n*-hexane:chloroform = 1:6:1 as eluent) to yield 10.7 g (81%) of a colorless liquid. ^{1}H NMR chemical shifts: δ 1.30 (s, 3H, $-CH_3$), 1.42–1.90 (m, 6H, $-O-CH_2-(CH_2)_3-$), 3.42–3.55 (m, 4H, $-CH_2-O-CH_2-$), 3.91 (t, 2H, $-CH_2-O-$Ph–), 4.33 and 4.50 (two d, 4H, two $-CH_2-$ in the oxetane ring), 5.01 (s, 2H, $-O-CH_2-$Ph), 6.83–7.46 (m, 9 aromatic protons).

3[[(4-Hydroxyphenyl)oxy]methyl]-3-methyloxetane (3), 3-[[[3-[(4-Hydroxyphenyl)oxy]propyl]oxy]methyl]-3-methyloxetane (12), 3-[[[4-[(4-Hydroxyphenyl)oxy]butyl]oxy]methyl]-3-methyloxetane (13), 3-[[[5-[(4-Hydroxyphenyl)oxy]pentyl]oxy]methyl]-3-methyloxetane (14), and 3-[[[6-[(4-Hydroxyphenyl)oxy]hexyl]oxy]methyl]-3-methyloxetane (15). All five compounds were pre-

pared by the same method. The synthesis of compound **14** is described below.

Sodium (7.46 g, 0.324 mol) was added rapidly but in small pieces to a hot solution of compound **10** (12.0 g, 0.03 mol) in 300 mL of anhydrous *t*-BuOH. The solution was heated to reflux for 24 h. After the sodium had completely reacted, a small amount of cold water was added, followed by the addition of a cold, dilute hydrochloric acid solution. The *t*-BuOH was removed in a rotovap, and the residue was extracted with dichloromethane. The collected dichloromethane solution was washed with water, dried over anhydrous magnesium sulfate, and then evaporated to dryness. The obtained product was purified by column chromatography (silica gel, ethyl acetate: *n*-hexane = 1:2 as eluent) to yield 5.60 g (62%) of white crystals. ^{1}H NMR chemical shifts: δ 1.30 (s, 3H, $-CH_3$), 1.42–1.90 (m, 6H $-O-CH_2-(CH_2)_3-$), 3.42–3.55 (m, 4H, $-CH_2-O-CH_2-$), 3.90 (t, 2H, $-CH_2-O-Ph-$), 4.33 and 4.50 (two d, 4H, two $-CH_2-$ in the oxetane ring), 6.78 (d, 4 aromatic protons).

Synthesis of Monomers IM–XIIIM. The monomers IM–XIIIM were synthesized by the same method. The preparation of monomer VIIIM is described below.

A solution of *trans-n*-propylcyclohexanecarboxylic acid (0.64 g, 3.75 mmol), *N,N*-dicyclohexylcarbodiimide (0.81 g, 3.93 mmol), compound **14** (1.00 g, 3.57 mmol), and 4-(dimethylamino)pyridine (0.044 g, 3.60 mmol) in dichloromethane (30 mL) was allowed to stir at room temperature until esterification was complete. The *N,N*-dicyclohexylurea was filtered. The obtained filtrate was washed three times with water and dried over anhydrous magnesium sulfate and the solvent evaporated in vacuum to give the crude product. The obtained product was purified by column chromatography (silica gel, ethyl acetate:*n*-hexane = 1:6 as eluent) to yield 0.87 g of a liquid. ^{1}H NMR chemical shifts: δ 0.80–2.20 (m, 25H, $-CH_3$, $-O-CH_2-(CH_2)_3-$, and $(-CH_2-CH_2)_2CH-C_3H_7$), 2.43 (tt, 1H, $-O-C(=O)-CH<$), 3.47 (m, 4H, $-CH_2-O-CH_2-CH_2-$), 3.93 (t, 2H, $-CH_2-O-Ph-$), 4.33 and 4.50 (two d, 4H, two $-CH_2-$ in the oxetane ring), 6.87 and 6.94 (two d, 4 aromatic protons).

The cyclohexane ring's methine proton, which is next to the carbonyl group, shows a chemical shift at about 2.43 ppm. This peak is split as a triplet of triplets and the coupling constant ($J_{axial-axial}$) is ca. 30 Hz. This means that the methine proton is at an axial position and the cyclohexane ring is in the trans form.[31]

Synthesis of Polyoxetanes IP–XIIIP. The synthesis of liquid crystalline polyoxetanes is also outlined in Schemes 1 and 2. All the polymers were synthesized by the same method. The preparation of polymer VIIIP is described below.

Dichloromethane was dried over calcium hydride and was distilled under nitrogen just prior to use. Freshly distilled boron trifluoride ether complex was used as an initiator. A solution of monomer VIIIM (0.432 g, 1 mmol) and dichloromethane (1 mL) was cooled to 0 °C under nitrogen and the initiator (2% mol with respect to monomer VIIIM) was then injected with a syringe. The reaction mixture was stirred at 0 °C for 24 h. After the reaction time, the polymers were separated and purified by several reprecipitations from dichloromethane solution into *n*-hexane. The absence of monomer was checked by ^{1}H NMR and GPC.

The results of ring-opening polymerization of oxetane monomers by BF_3·OEt_2 as an initiator are summarized in Table 1. All monomers gave reasonable yields in the polymerization. Figure 1 presents the representative ^{1}H and ^{13}C NMR spectra of polymer IIP. The assignment of the carbon signals of polymers has been made on the basis of DEPT (distortionless enhancement by polarization transfer) spectra (curve B and C). The chemical shifts of polymer IIP are reported as follows: ^{1}H NMR ($CDCl_3$, TMS, ppm) δ 0.80–2.20 (m, 21H, $^1CH_3-$, $^6CH_2-$ and $(-CH_2-CH_2)_2CH-C_3H_7$), 2.40 (tt, 1H, $-O-C(=O)-CH<$), 3.15–3.23 (m, 6H, $CH_3-C(-CH_2)_2-CH_2-O-$), 3.84 (t, 2H, $-O-^5CH_2-$), 3.94 (t, 2H, $-^7CH_2-O-Ph-$), 6.80 and 6.90 (two d, 4 aromatic

Table 1. Polymerization of Monomers by Boron Trifluoride Ether Complex[a–c]

monomer	n[d]	m[d]	yield, %	$10^{-3}\bar{M}_w$	$10^{-3}\bar{M}_n$	$\bar{M}_w/\bar{M}_n$	$\overline{DP}$[e]
IM	0	5	73.6	54.5	28.0	1.95	75
IIM	3	3	72.4	64.7	47.9	1.35	118
IIIM	3	4	68.5	56.5	44.0	1.28	105
IVM	3	5	52.3	67.7	51.9	1.30	120
VM	4	3	67.6	40.5	32.1	1.26	77
VIM	4	4	70.4	82.2	59.0	1.39	136
VIIM	4	5	51.7	40.9	32.9	1.24	74
VIIIM	5	3	62.4	27.6	22.1	1.25	51
IXM	5	4	68.5	29.6	24.5	1.21	55
XM	5	5	70.3	31.9	26.3	1.21	57
XIM	6	3	65.4	26.4	20.9	1.26	47
XIIM	6	4	70.6	28.6	24.5	1.17	53
XIIIM	6	5	67.6	31.2	26.6	1.17	56

[a] Solvent: CH_2Cl_2. Reaction temperature: 0 °C. Reaction time: 24 h. [b] The concentration of monomer in CH_2Cl_2: 1.0 M. [c] [Monomer]:[BF_3·OEt_2] = 50:1. [d] n and m according to Scheme 1. [e] $\overline{DP}$: degree of polymerization.

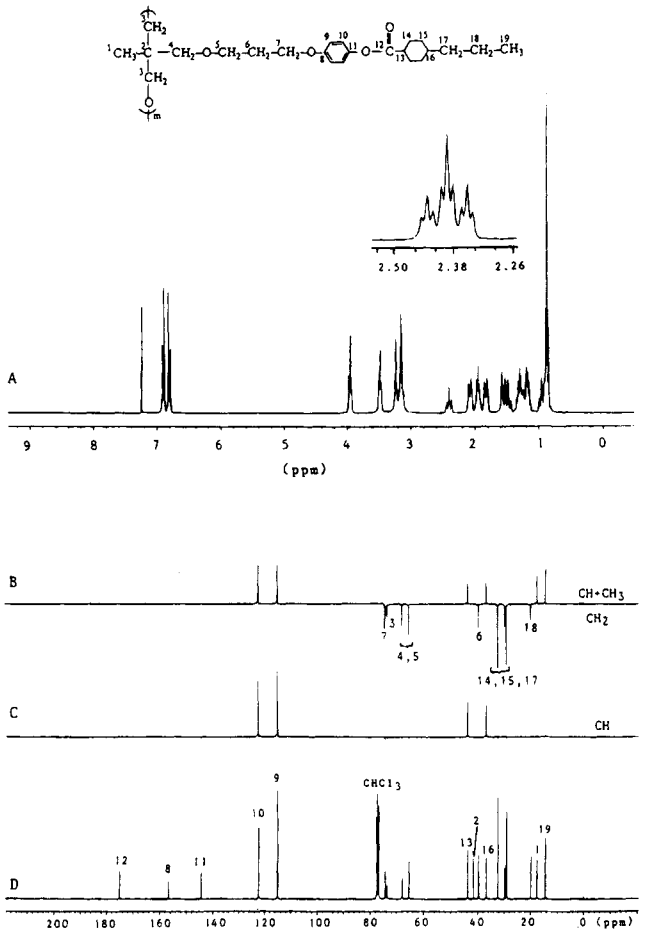

Figure 1. (A) ^{1}H NMR spectrum, (b) ^{13}C NMR DEPT (135) spectrum, (C) ^{13}C NMR DEPT (90) spectrum, (D)^{13}C NMR spectrum for polymer IIP.

Table 2. Thermal Transitions and Thermodynamic Parameters of Monomers IM–XIIIM

monomer	n^a	m^a	phase transitions, °C (corresponding enthalpy changes, kcal/mol)[b] heating / cooling
IM	0	5	K 93.7 (2.83) I / I 63.0 (2.62) K
IIM	3	3	K 52.1 (8.30) I / I -39.3 (0.90) K
IIIM	3	4	K 46.8 (7.90) I / I -26.3 (0.65) K
IVM	3	5	K 50.8 (7.61) I / I -1.2 (5.76) K
VM	4	3	K 40.7 (6.54) I / I 3.8 (0.13) N -20.0 (0.10) K
VIM	4	4	K 49.1 (10.0) I / I 6.4 (0.06) N -17.7 (1.22) K
VIIM	4	5	K 51.8 (9.51) I / I 21.8 (0.17) N -9.3 (0.46) K_1 -38.2 (1.40) K_2
VIIIM	5	3	K_1 2.9 (2.54) K_2 24.6 (4.87) I / I -19.6 (–)[c] K_2 25.3 (1.54) K_1
IXM	5	4	K 28.8 (5.72) I / I -3.7 (2.55) K
XM	5	5	K 35.6 (6.44) I / I 15.4 (1.33) K_1 -14.7 (2.89) K_2
XIM	6	3	K 27.6 (6.09) I / I 11.2 (0.15) N -27.2 (0.42) K
XIIM	6	4	K 19.6 (8.41) I / I 12.7 (0.13) N -10.1 (0.65) K
XIIIM	6	5	K 27.3 (7.25) I / I 25.3 (0.15) N 6.2 (0.68) K

[a] n and m according to Scheme 2. [b] K = crystalline, N = nematic, I = isotropic. [c] Overlapped transition.

protons); ^{13}C NMR ($CDCl_3$, TMS, ppm) δ 14.33 (C19), 17.47 (C1), 19.86 (C18), 28.95, 29.57, 32.19 (C14, C15, C17), 36.56 (C16), 39.41 (C6), 41.28 (C2), 43.49 (C13), 65.29, 67.79 (C4, C5), 73.45 (C3), 74.15 (C7), 114.88 (C9), 122.19 (C10), 144.16 (C11), 156.49 (C8), 174.96 (C12).

The molecular weights of these polymers were determined by GPC using a calibration based on polystyrene standards and therefore have only a relative meaning. The obtained polymers show very narrow molecular weight distributions. The calculated degrees of polymerization based on GPC results are higher than 47 for all polymers. It is well-documented that the thermal transitions of a side-chain liquid crystalline polymer are usually molecular-weight independent if its degree of polymerization reaches such a high value.[35]

Results and Discussion

The thermal behavior of all monomers is reported in Table 2. Monomers IM–IVM, which contain respectively a spacer length less than four methylene units, show no mesomorphic behavior. This could be due to the bulky oxetane group. Monomers VM–VIIM that contain four methylene units in their spacers exhibit only a monotropic nematic phase. They display respectively a characteristic schlieren nematic texture. To our surprise, monomers VIIIM–XM that contain five methylene units in their spacers, show also no mesophase. Besides five methylene units, monomers VIIIM–XM contain respectively also a methylene oxide and an oxide unit in their spacers, i.e., there are eight atoms in a spacer. However they do not reveal any mesophase. It seems that the odd–even effect plays also a very important role in the formation of a mesophase in addition to the effect of a bulky oxetane group. Monomers XIM–XIIIM that contain six methylene units in their spacers reveal again a monotropic nematic phase. Furthermore, let us consider the effect of the length of the terminal alkyl group on the mesomorphic properties exhibited by the monomers. According to the data reported in Table 2, the length of the terminal alkyl group does not affect the nature of the mesophases formed by the monomers. However, it does affect the thermal stability of the mesophases. A monomer with a longer terminal alkyl group tends to form a wider mesomorphic temperature range.

Table 3. Phase Transitions and Phase Transition Enthalpies of Polymers IP–XVIP

polymer	m^a	n^a	phase transitions, °C (corresponding enthalpy changes, kcal/mru)[b] heating / cooling
IP	0	5	G 11.9 S_X 97.8 (1.16) S_A 125.8 (0.31) I / I 125.2 (0.02) S_A 89.5 (0.96) S_X
IIP	3	3	G 12.0 S_A 33.1 (0.56) N 43.0 (0.03) I / I 35.3 (0.03) N 19.8 (0.21) S_A
IIIP	3	4	G 10.0 S_X 34.9 (–)[c] S_A 52.0 (0.35) N 54.3 (0.01) I / I 53.0 (0.01)[c] N 48.0 (–)[c] S_A 27.3 (0.51) S_X
IVP	3	5	G 21.0 S_X 65.5 (–)[c] S_A 75.0 (1.17) N 76.2 (–)[c] I / I 75.6 (–)[c] N 72.7 (0.44) S_A 44.7 (0.22) S_X
VP	4	3	G -0.6 S_A 57.0 (0.01) N 74.5 (0.01) I / I 73.4 (0.01) N 40.0 (0.01) S_A
VIP	4	4	G 2.1 S_X 65.5 (0.05) S_A 83.0 (0.01) N 86.4 (0.01) I / I 84.2 (0.01) N 76.0 (0.01) S_A 40.4 (0.02) S_X
VIIP	4	5	G 24.1 S_X 60.4 (0.18) S_A 94.2 (–)[c] N 105.9 (0.66) I / I 102.1 (–)[c] N 89.7 (0.62) S_A 55.4 (0.20) S_X
VIIIP	5	3	G 11.7 S_X 38.9 (0.02) S_A 53.8 (0.03) N 71.9 (0.03) I / I 68.2 (0.02) N 50.1 (0.04) S_A 34.0 (0.01) S_X
IXP	5	4	G 8.3 S_X 38.1 (0.12) S_C 56.2 (0.14) S_A 89.7 (0.07) I / I 85.6 (0.06) S_A 51.7 (0.06) S_C 34.0 (0.06) S_X
XP	5	5	G 28.1 S_X 51.8 (0.04) S_B 65.4 (0.29) S_A 104.9 (0.78) I / I 100.4 (0.78) S_A 61.4 (0.33) S_B 47.7 (0.10) S_X
XIP	6	3	G 3.8 S_X 36.9 (0.54) S_A 84.0 (0.48) N 87.6 (–)[c] I / I 83.9 (–)[c] N 81.1 (0.51) S_A 30.8 (0.43) S_X
XIIP	6	4	G 1.9 S_X 44.1 (1.09)[c] S_C 56.2 (–) S_A 98.5 (0.65) I / I 94.0 (0.66) S_A 52.5 (–)[c] S_C 40.0 (1.15) S_X
XIIIP	6	5	G 22.4 S_X 57.4 (0.07) S_B 68.7 (0.03) S_A 115.0 (0.98) I / I 110.5 (0.85) S_A 65.4 (0.31) S_B 54.5 (0.08) S_X
XIVP[e]	12	3	G 34.1 S_X 67.9 (0.11) S_B 73.9 (0.90) S_A 112.2 (1.32) I / I 107.3 (1.42) S_A 70.3 (–)[c] S_B 64.2 (1.09) S_X
XVP[e]	12	4	G 36.6 S_X 75.6 (0.22) S_B 83.2 (0.99) S_A 118.2 (1.39) I / I 112.9 (1.47) S_A 79.5 (0.92) S_B 71.5 (0.02) S_X
XVIP[e]	12	5	G 43.0 S_X 74.7 (0.21) S_B 93.3 (1.04) S_A 126.3 (1.50) I / I 120.6 (1.59) S_A 89.6 (1.06) S_B 70.7 (0.23) S_X

[a] According to Scheme 2. [b] mru = mole repeating unit (for polymers). [c] Overlapped transition. [g] G = glassy, K = crystalline, I = isotropic phase, N = nematic phase, S_A = smectic A phase, S_B = smectic B phase, S_C = smectic C phase, S_X = undefined smectic phase, prabable a smectic G phase. [e] Data obtained from ref 36.

Table 3 reported the thermal transition and thermodynamic parameters of polymers IP–XIIIP. All polymers reveal liquid crystalline phases. The phase assignment was conducted by both optical polarizing microscopy and X-ray diffraction measurements. Polymer IP that contains no methylene unit in the spacers

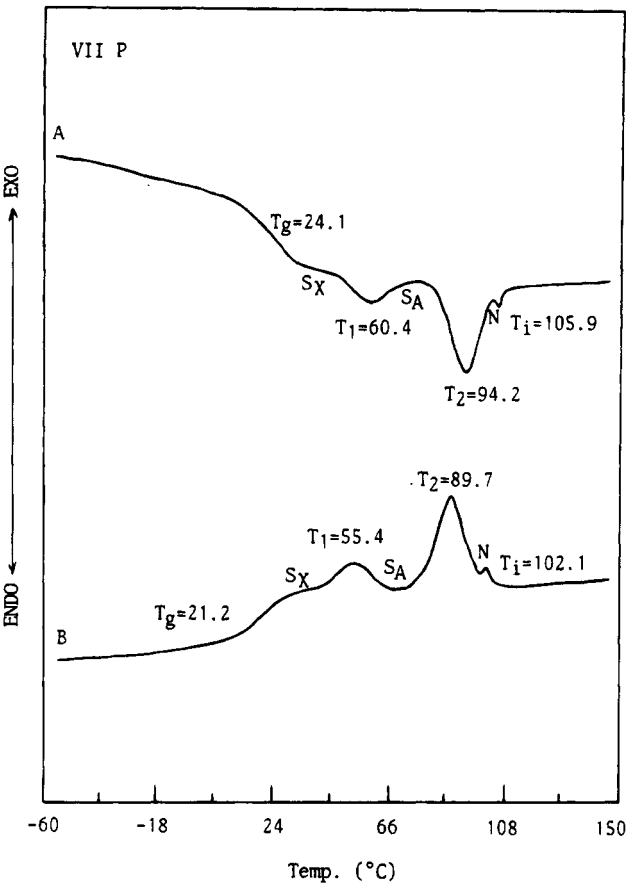

Figure 2. DSC thermograms of VIIP (10 °C/min): (A) second heating scan; (B) cooling scan.

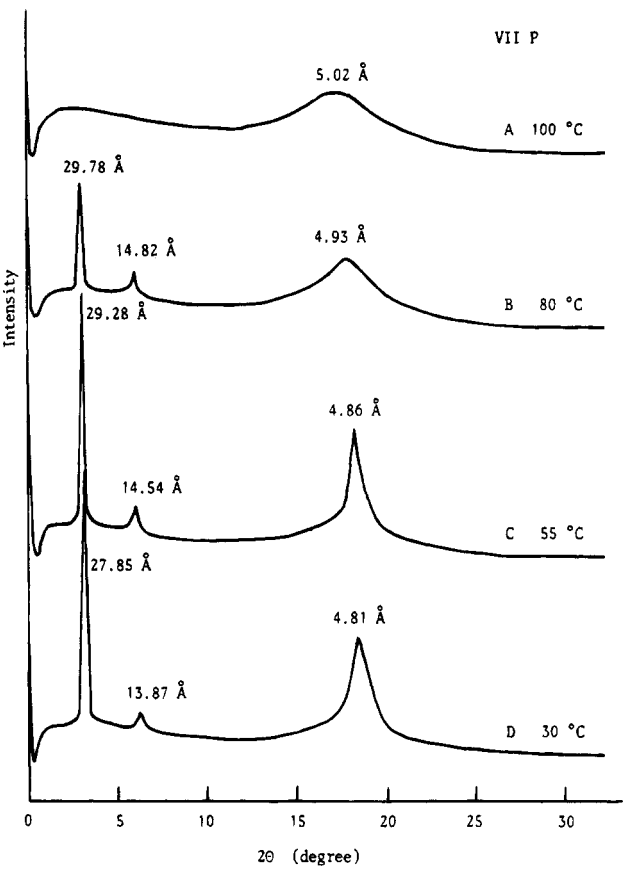

Figure 3. Temperature-dependent X-ray measurements for polymer VIIP at (A) 100, (b) 80, (C) 55, and (D) 30 °C.

exhibits enantiotropic smectic A and an undefined smectic phase. Among polymers IIP–IVP that contain three methylene units in their spacers, polymer IIP presents enantiotropic nematic and smectic A phases, while both polymers IIIP and IVP exhibit enantiotropic nematic, smectic A, and an undefined smectic phase. Polymers VP–VIIP that contain four methylene units in their spacers, show mesomorphic behavior very similar to that of their corresponding polymers IIP–IVP. It seems that the nature of the mesophase depends on the length of the terminal alkyl groups. Both polymers IIP and VP containing a propyl end group, revealing nematic and smectic A phases, while the other four polymers that contain either a butyl or a pentyl end group exhibit nematic, smectic A, and an undefined smectic phase. Figure 2 illustrates the representative DSC traces of polymer VIIP. On the heating scan (curve A), it shows a glass transition temperature (T_g) at 24.1 °C followed by an undefined smectic to smectic A phase transition at 60.4 °C, a smectic A to nematic phase transition at 94.2 °C, and a nematic to isotropic phase transition at 105.9 °C. The cooling scan (curve B) looks almost identical to the heating scan, except that a very small supercooling (less than 5 °C) is observed for all three exothermic transitions. Figure 3 presents the temperature-dependent X-ray diffraction diagrams obtained from the powder sample of VIIP at 100, 80, 55, and 30 °C. Curve A shows only a diffuse reflection at about 5.02 Å that corresponds to the lateral spacing of mesogenic side groups. It indicates the formation of a nematic phase. The optical polarizing micrograph (Figure 4A) also reveals a characteristic nematic texture. When the measuring temperature has been lowered to 80 °C, a sharp first-order reflection at 29.78 Å and a second-order reflection at 14.82 Å (associated with the smectic layers) are observed (curve B). The optical polarizing micrograph (Figure 4B) reveals a focal-conic fan texture for polymer VIIP in this temperature range. Both results are consistent with a smectic A structure. When the measuring temperature has been further cooled to 30 °C, the d spacing of the first-order reflection decreases from 29.78 to 27.85 Å and a sharp wide angle reflection is observed (curve D). The optical polarizing micrograph (Figure 4C) shows a higher ordered smectic texture. These results indicate the formation of a tilted smectic phase, prabably a smectic G phase. The detailed structure of this smectic phase should be further studied by X-ray diffraction patterns of an aligned monodomain sample.

Among polymers VIIIP–XP that contain five methylene units in their spacers, polymer VIIIP exhibits enantiotropic nematic, smectic A, and an undefined smectic phase, polymer IXP reveals enantiotropic smectic A, smectic C, and an undefined smectic phase, while polymer XP presents enantiotropic smectic A, B, and an undefined phase. Polymers XIP–XIIIP that contain six methylene units in their spacers show mesomorphic behavior very similar to that of their corresponding polymers VIIIP–XP. Again it demonstrates that the nature of the mesophase depends on the length of the terminal alkyl groups. Both polymers VIIIP and XIP with a propyl end group exhibit enantiotropic nematic, smectic A, and an undefined smectic phase. Their X-ray diffraction patterns and optical polarizing micrographs are very similar to those of polymer VIIP. Both polymers IXP and XIIP with a butyl end group reveal enantiotropic smectic A, C, and an undefined phase. Figure 5 presents the DSC traces of polymer XIIP. It shows respectively a glass transition and three thermal transitions on both heating and cooling scans. The

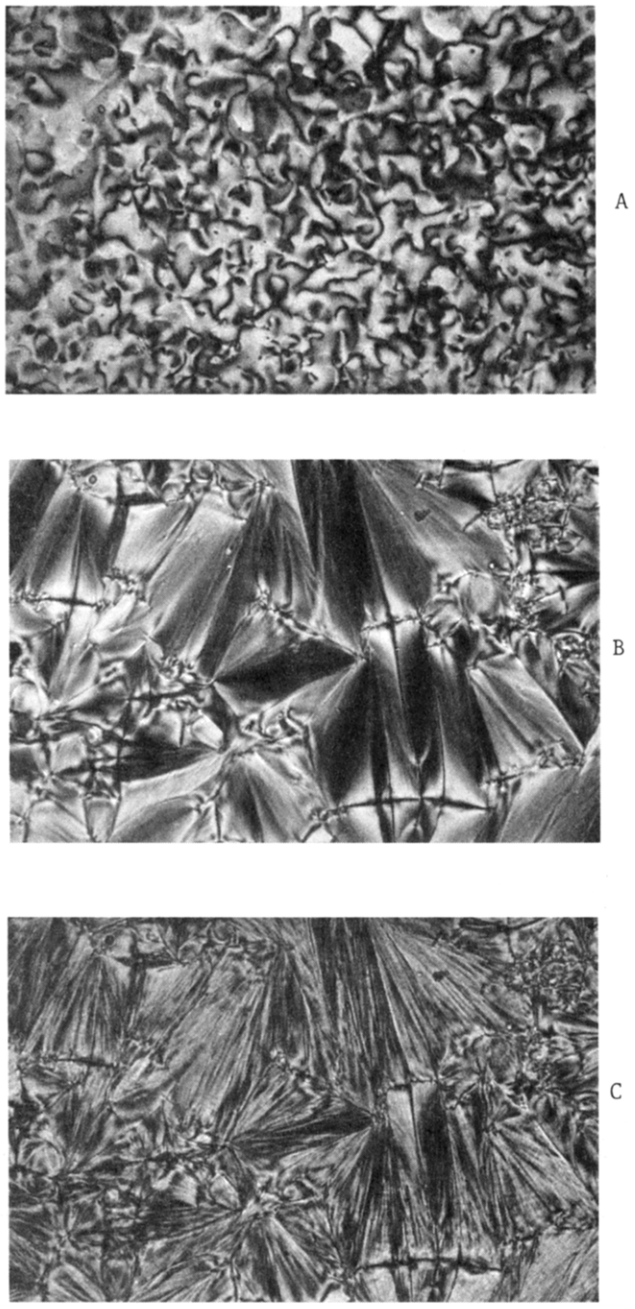

Figure 4. Optical polarizing micrographs displayed by VIIP: (A) N texture obtained after cooling from isotropic phase to 101 °C; (B) S_A texture obtained after cooling to 85 °C; (C) higher ordered smectic texture obtained after cooling to 31 °C.

temperature-dependent X-ray diffraction diagrams obtained from a powder sample of XIIP at 85, 50, and 25 °C are shown in Figure 6. Curve A shows a diffuse wide-angle reflection at 4.93 Å (associated with the lateral spacing of mesogenic side groups) and a sharp first-order reflection at 28.89 Å and a second-order reflection at 14.49 Å (both associated with the smectic layers) in the small-angle region. The optical polarizing micrograph reveals a focal-conic fan texture for polymer XIIP at this temperature range. Both results are consistent with a smectic A structure. When the measuring temperature has been lowered from 85 to 50 °C, the *d* spacing of the first-order reflection decreases from 28.89 to 24.48 Å (curve B). This gives strong evidence for the formation of the tilted smectic C phase. This result is also in agreement with the optical polarizing microscopic observation that reveals a broken fan

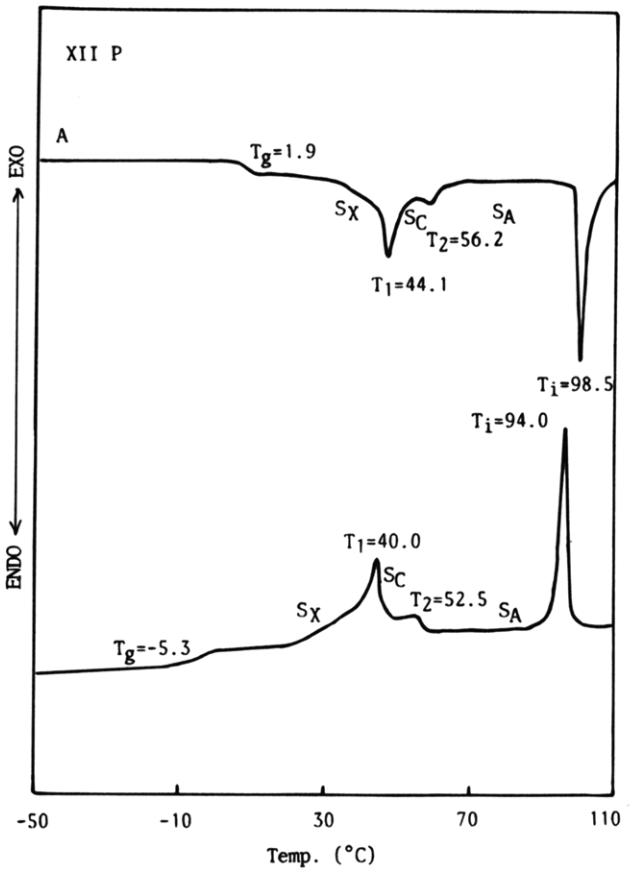

Figure 5. DSC thermograms of XIIP (10 °C/min): (A) second heating scan; (B) cooling scan.

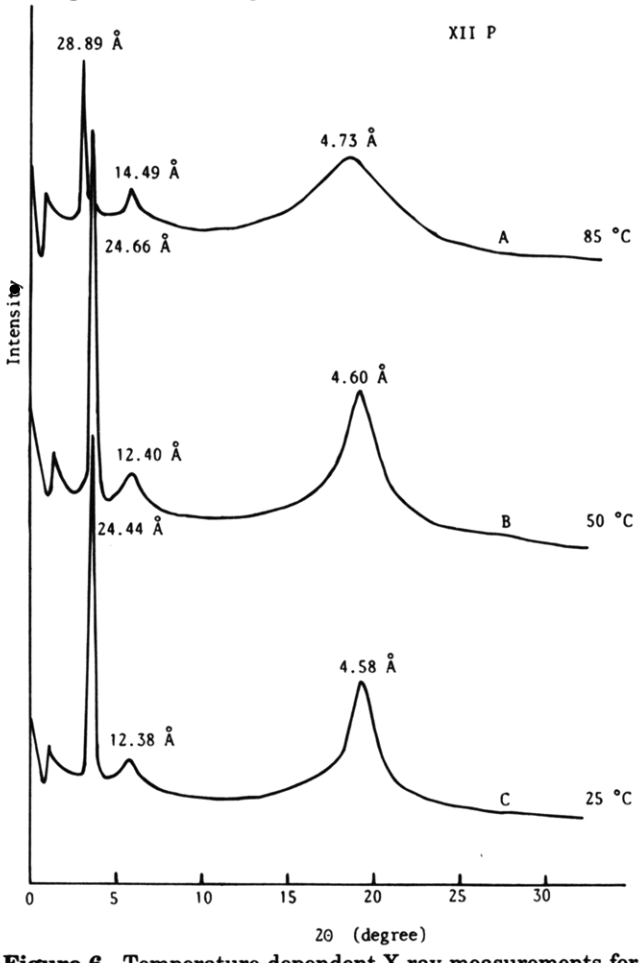

Figure 6. Temperature-dependent X-ray measurements for polymer XIIP at (A) 85, (B) 50, and (C) 25 °C.

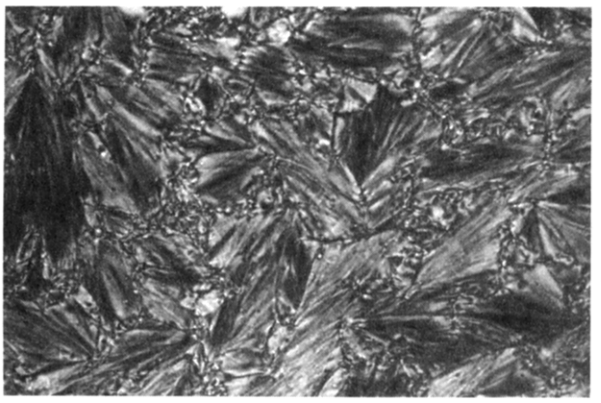

Figure 7. Optical polarizing micrograph displayed by XIIP: S_C texture obtained after cooling from isotropic phase to 50 °C.

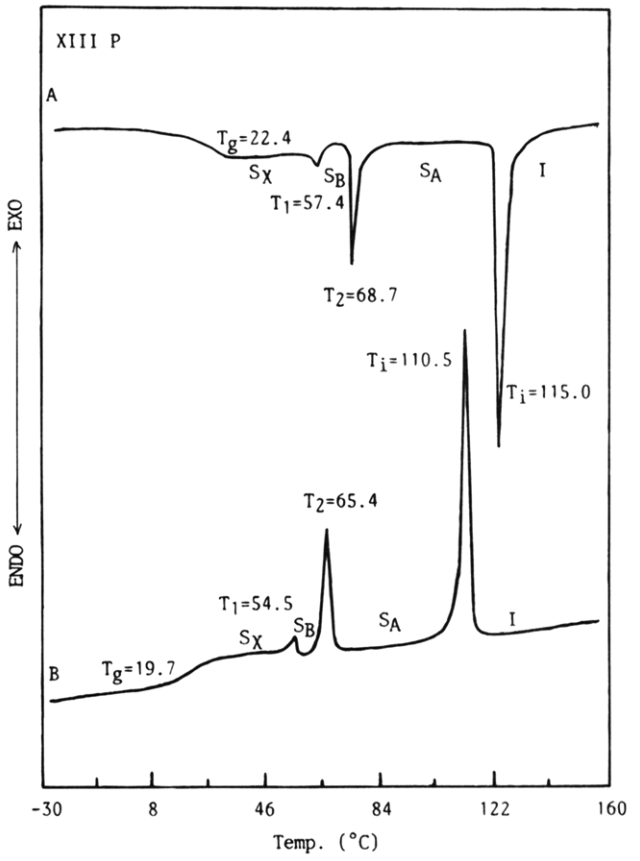

Figure 8. DSC thermograms of XIIIP (10 °C/min):(A) second heating scan; (B) cooling scan.

texture (Figure 7). When the measuring temperature has been further cooled to 25 °C, the *d* spacing of the first-order reflection remains at the same value and the wide-angle reflection becomes very sharp. The texture obtained at this temperature looks identical to that of Figure 4C. The results indicate the formation of a tilted smectic phase. Both polymers XP and XIIIP with a pentyl end group show enantiotropic smectic A, B, and an undefined phase. Figure 8 depicts the DSC traces of polymer XIIIP. It shows respectively a glass transition and three thermal transitions on both heating and cooling scans. Figure 9 presents the temperature-dependent X-ray diffraction diagrams obtained from a powder sample of XIIIP at 95, 65, 55, and 35 °C. Curve A shows a diffuse reflection at 4.93 Å at the wide-angle region, a sharp first-order reflection at 30.99 Å, and a second-order reflection at 15.58Å at small-angle region.

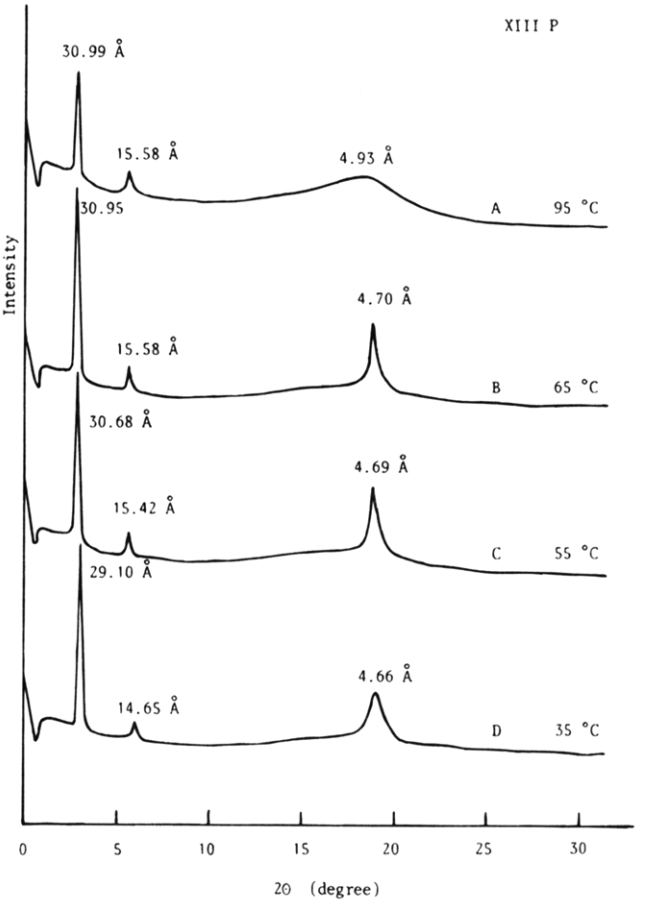

Figure 9. Temperature-dependent X-ray measurements for polymer XIIIP at (A) 95, (B) 65, (C) 55, and (D) 35 °C.

Figure 10. Optical polarizing micrograph displayed by XIIIP: S_B texture obtained after cooling from isotropic phase to 66.5 °C.

The optical polarizing micrograph reveals a focal-conic fan texture for polymer XIIIP at this temperature range. Both results are consistent with a smectic A structure. When the measuring temperature has been lowered from 95 to 65 °C, the wide-angle reflection becomes very sharp (curve B). The optical polarizing micrograph (Figure 10) reveals some arc lines across the back of the fan at the transition temperature region (near 66.5 °C). The arc lines will disappear when the temperature is further cooled. These results indicate the formation of a smectic B phase.[37] When the measuring temperature has been further cooled to 35 °C, the *d* spacing of the first-order reflection decreases from 30.95 to 29.10 Å. The texture obtained at this temperature looks identical to that of Figure 4C. The results indicate the formation of a tilted smectic phase. Polymers XIVP–XVIP that

contain twelve methylene units in their spacers, show completely the same mesomorphic behavior with polymers XP and XIIIP.

The experimental data reported in Table 3 demonstrate that all polymers show polymorphism of mesophases. In each series of polymers which contain the same terminal group, the isotropization temperature first decreases and then increases with increasing spacer length. Furthermore, the spacer length can affect also the nature of the mesophases formed. The polymers with shorter spacer lengths (n = 3, 4) form also a nematic phase besides the other two smectic phases, while those with longer spacer lengths ($n \geq 5$) form only three smectic phases.

Conclusions

A new series of side-chain liquid crystalline polyoxetanes containing 4-(alkanyloxy)phenyl *trans*-4-alkylcyclohexanoate side groups are synthesized. The obtained polymers reveal polymorphism of mesophases. Both spacer length and terminal alkyl length have a profound effect on the nature and thermal stability of the mesophases. Although the polyoxetane backbone is expected to be more flexible than the polymethacrylate backbone, all the obtained polymers do not undergo side-chain crystallization even if twelve methylene units are used to connect the polymer backbone and the mesogenic units. This results could be due to the cyclohexane based mesogenic units that, as illustrated in our previous studies,[32-34] exhibits conformational isomerism.

Acknowledgment. The authors are grateful to the National Science Council of the Republic of China for financial support of this work (Grants NSC-83-0405-E009-010).

References and Notes

(1) Ciferri, A., Krigbaum, W. R., Eds. *Polymer Liquid Crystals*; Academic Press: New York, 1982.
(2) Chapoy, L. L., Eds. *Recent Advances in Liquid Crystalline Polymers*; Elsevier: London and New York, 1985.
(3) Blumstein, A., Eds. *Polymeric Liquid Crystals*; Plenum: New York, 1985.
(4) McArdle, C. B., Eds. *Side Chain Liquid Crystal Polymers*; Blackie: Glasgow and London, 1989.
(5) Jones, B. A.; Bradshaw, J. S.; Nishioka, M.; Lee, M. L. *J. Org. Chem.* **1984**, *49*, 4947.
(6) Apfel, M. A.; Finkelmann, H.; Janini G. M.; Lamb R. J.; Luhmann, B. H.; Price, A.; Roberts, W. U.; Shaw, T. J.; Smith, C. A. *Anal. Chem.* **1985**, *57*, 651.
(7) Bradshaw, J. S.; Schregenberg, C.; Karen H. C.; Markides, K. E.; Lee M. L. *J. Chromatogr.* **1986**, *358*, 95.
(8) Coles, H. J.; Simon, R. *Polymer* **1985**, *26*, 1801.
(9) Goozner, R. F.; Finkelmann, H. *Makromol. Chem.* **1985**, *186*, 2407.
(10) Eich, M.; Wendorff, J. H.; Reck B.; Ringsdorf, H. *Makromol. Chem. Rapid. Commun.* **1987**, *8*, 59.
(11) Eich, M.; Wendorff, J. H. *Makromol. Chem. Rapid. Commun.* **1987**, *8*, 467.
(12) Armitage, D.; Thackara, J. I.; Eades, W. D. *Liq. Cryst.* **1989**, *5*, 1389.
(13) Gray, G. W.; Hawthorne, W. D.; Hill, J. S.; Lacey, D.; Lee, M. S. K.; Nestor, G.; White, M. S. *Polymer* **1989**, *30*, 964.
(14) Ortler, R.; Brauchle, C.; Miller, A.; Riepl, G. *Makromol. Chem. Rapid. Commun.* **1989**, *10*, 189.
(15) Natansohn, A.; Xie, S.; Rochon, P. *Macromolecules* **1992**, *25*, 5531.
(16) Perec, V.; Tomazos, D. *Adv. Mater.* **1992**, *4*, 549.
(17) Tuan, P. A.; Kostromin, S. G.; Shibaev, V. P. *Polym. Bull.* **1992**, *29*, 49.
(18) Fujishiro, K.; Pajerski, A. D.; Lenz, R. W. *Liq. Cryst.* **1992**, *12*, 417.
(19) Fujishiro, K.; Lenz, R. W. *Liq. Cryst.* **1992**, *12*, 561.
(20) Tuan, P. A.; Kostromin, S. G.; Shibaev, V. P. *Polym. Bull.* **1993**, *30*, 249.
(21) Akiyama, E.; Nagase, Y. *Makromol. Chem., Rapid Commun.* **1993**, *14*, 251.
(22) Kawakami, Y.; Takahashi, K.; Hibino, H. *Macromolecules* **1991**, *24*, 4531.
(23) Kawakami, Y.; Takahashi, K. *Polym. Bull.* **1991**, *25*, 439.
(24) Kawakami, Y.; Takahashi, K.; Nishiguchi, S.; Toida, K. *Polym. Int.* **1993**, *31*, 35.
(25) Komiya, Z.; Pugh, C.; Schrock, R. R. *Macromolecules* **1992**, *25*, 6586.
(26) Pugh, C.; Schrock, R. R. *Macromolecules* **1992**, *25*, 6593.
(27) Komiya, Z.; Schrock R. R. *Macromolecules* **1993**, *26*, 1387.
(28) Komiya, Z.; Schrock, R. R. *Macromolecules* **1993**, *26*, 1393.
(29) Kim, S. H.; Lee, H. J.; Jin, S. H.; Cho, H. N.; Choi, S. K. *Macromolecules* **1993**, *26*, 846.
(30) Hsu, C. S.; Lu, Y. H. *Polym. Bull.* **1991**, *25*, 169.
(31) Hsu, C. S.; Lu, Y. H. *J. Polym. Sci., Polym. Chem.* **1991**, *29*, 977.
(32) Hsu, C. S.; Rodriguez-Parada, J. M.; Percec, V. *Makromol. Chem.* **1987**, *188*, 1017.
(33) Hsu, C. S.; Rodriguez-Parada, J. M.; Percec, V. *J. Polym. Sci., Polym. Chem.* **1987**, *25*, 2425.
(34) Hsu, C. S.; Percec, V. *Makromol. Chem.* **1988**, *189*, 1141.
(35) Percec, V.; Pugh, C. In *Side Chain Liquid Crystal Polymers*; McArdle, C. B.; Ed.; Chapman and Hall: New York, 1989; p 53.
(36) Hsu, C. S.; Lu, Y. H.; Chang, H. L. *Polym. Bull.*, in press.
(37) Gray, G. W.; Goodby J. W. *Smectic Liquid Crystals, Texture and Structures*; Leonard Hill: Glasgow and London, 1984; p 39.

MA941155S